JOURNAL OF SOLID STATE CHEMISTRY 29, 109–115 (1979)

Manifestation of Phonons in $TlMnCl_3$ Absorption Spectrum

M. M. KOTLYARSKII

L. V. Kirenskii Institute of Physics, USSR Academy of Sciences, Krasnoyarsk, 660036, USSR

Received July 17, 1978

The temperature dependence of the $TlMnCl_3$ absorption spectrum is investigated in the region of the *C*- and *D*-group bands. It is shown that the excitation–magnon–phonon process is the fundamental mechanism of light absorption in the region of the *C* group of $TlMnCl_3$, contrary to $K(Rb)MnF_3$. In the latter case and in the *D* group of $TlMnCl_3$ the excitation–magnon mechanism is the main mechanism. The peculiarities of the absorption spectrum are discussed in terms of the Franck–Condon principle. The frequencies of magnons and phonons are determined.

Introduction

The study of the optical absorption spectra of $AMnF_3$ compounds (A = Rb, Cs, K) (*1–4*) shows that the exciton–magnon (EM) process is the main process responsible for the fine structure of the absorption spectrum in magnetically ordered crystals. This mechanism of light absorption permits one to explain large intensities of the doubly forbidden *d–d* transitions in Mn^{2+} ion compounds and to understand intensity distribution versus frequency for all *d–d* transitions. The interaction of phonons with excitons and magnons causes the appearance of weak exciton–phonon (EP) or exciton–magnon–phonon (EMP) bands. In some cases such bands form an electron–vibrational series. The frequencies of such series may be described by the following relation (*3, 4*),

$$\nu_{n_k} = \nu_0 + n_k \nu_k, \qquad (1)$$

where $n_k = 0, 1, 2, \ldots$, ν_{n_k} is the frequency of the n_k member of the series, ν_0 is the frequency of the series origin band, and ν_k is the boundary frequency of the k optical branch.

In the present paper we investigate the role of phonons in the formation of the $TlMnCl_3$ absorption spectrum. This work extends our previous study of the absorption spectrum of $TlMnCl_3$ (*5*) by use of a high-resolution spectrograph which permits us to see a number of new features in the fine structure of the $TlMnCl_3$ absorption spectrum.

$TlMnCl_3$ has an ideal perovskite structure (O_h^1) with $a_0 = 5.04$ Å at the temperature $T = 300$°K (*6*). On cooling, the crystal undergoes a number of structural phase transitions in analogy with $KMnF_3$ (*6*). The Néel temperature of $TlMnCl_3$ is $T_N = 113$°K (*7*).

Experimental Details

Optical measurements were performed in unpolarized light in the temperature range from 4.2 to 77°K with a ДФС−8 grating spectrograph with 3 Å/mm dispersion in first

0022-4596/79/070109-07$02.00/0

order. The temperature was obtained as described in (*8*). The spectra were recorded with the ИФО−451. The positions of the bands were determined with an accuracy of 1 cm^{-1} for sharp bands and 5 cm^{-1} for broad bands. Single crystals of $TlMnCl_3$ were grown by B. V. Beznosikov from the melt in quartz ampoules at 500°C by the Bridgman technique. Three samples with thicknesses $d = 0.35$, 1.5, and 12.6 mm were investigated.

Results and Discussion

The optical absorption spectrum of $TlMnCl_3$ in the region from 3000 to 6000 Å contains six groups of bands, as is typical for divalent manganese compounds. The energies of the centers of these groups are shown in Table I. The differences between the frequencies of identical transitions for $TlMnCl_3$ and isostructural $KMnF_3$ are also shown for comparison. A and B groups form wide and diffusive distributions (half-widths from 300 to 500 cm^{-1}) with no fine structure. As for E and F groups we indicate the centers of the groups of bands because their fine structures have low resolution even for the thinnest sample with $d = 0.35$ mm. The absorption spectrum of $TlMnCl_3$ in comparison with $KMnF_3$ (Table I) is displaced to the low-frequency region. The same result has been obtained for isostructural compounds $RbMnCl_3$ and $CsMnF_3$ (*9*). This displacement proves that the crystal field in chlorides is smaller than that in fluorides (*10*).

The absorption spectrum of $TlMnCl_3$ in the region of the C and D groups is shown in Figs. 1 and 2. In Table II the energies of C and D groups of lines at 4.2°K are compiled along with their assignments (ν_E^{av} and ν_D^{av} are the frequencies of the centers of gravity for C_0^a, C_0^b and D_1, D_2 bands, respectively). An evaluation of the band intensities shows that the absorption spectra of both groups are formed mainly by electric–dipole bands. C_0^a, C_0^b, C_3 and D_1, D_2 (the insert in Fig. 2) are magnito–dipole pure excitonic (PE) bands. The appearance of D_1 and D_2 bands is obviously caused by the influence of tetrahedral components of the crystal field on the $^4T_{2g}$ (^4D) transition (*11*).

The temperature dependence has been investigated for the bands which do not broaden and disappear on warming. The complete disappearance of the $TlMnCl_3$ fine structure occurs at temperatures $T \approx 60$°K, which is essentially lower than T_N. We have not succeeded in observing the temperature

TABLE I

ABSORPTION SPECTRUM OF $TlMnCl_3$ AT 4.2°K IN THE REGION OF 3000–6000 Å

Excited state of Mn^{2+} ion transition from ground state $^6A_{1g}$ (^6S)	Group (band)	Frequency (cm^{-1})	$\Delta\nu$($KMnF_3$–$TlMnCl_3$) (cm^{-1})
$^4T_{1g}(^4G)$	A	19,360	1,410
$^4T_{2g}(^4G)$	B	22,520	Data absent
$^4E_g{}^4A_{1g}(^4G)$	$C(\nu_E^{av})$	23,573	1,520
$^4T_{2g}(^4D)$	$D(\nu_D^{av})$	26,630	1,145
$^4E_g(^4D)$	E	28,200	1,860
$^4T_{1g}(^4P)$	F	29,870	2,320

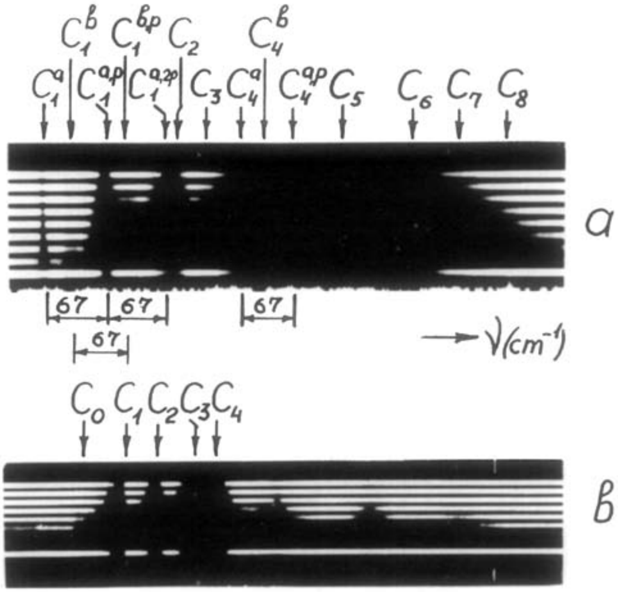

FIG. 1. (a) Absorption spectrum of $TlMnCl_3$ in the region of the C-group bands at 4.2°K; $d = 0.34$ mm. (b) Absorption spectrum of $KMnF_3$ in the region of the C-group bands at 4.2°K; $d = 1.5$ mm [from (*3*)].

dependence of the PE bands because of their overlap with the edges of high-intensity EMP bands. The temperature displacements of the C_1^a, C_1^b, $C_1^{a,p}$, $C_1^{b,p}$, and D_3 bands may be described by the equation (*4*)[1]

$$\nu(T) = \nu_0 + \beta B_{5/2}(T/T_N).$$

This relation is typical for the magnon participating in the creation of the band. C_h is the "hot" magnon sideband. It is not observed at 4.2°K and appears in the spectrum at $T \geqq 32$°K. The temperature dependence of the intensity of the D group is shown in Fig. 3.

In order to understand the nature of lines we use the temperature dependence of the bands, their shapes, characteristic frequency intervals, and the analogy with the previously studied $KMnF_3$ and $RbMnF_3$ (*3, 11–16*). The following magnon frequencies have

[1] Notations as in (*4, 13*).

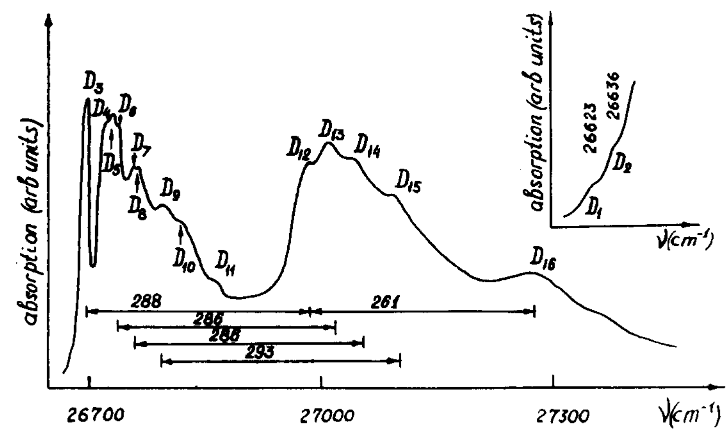

FIG. 2. Absorption spectrum of $TlMnCl_3$ in the region of the D-group bands at 4.2°K; $d = 1.52$ mm. Pure excitonic bands D_1 and D_2 are shown in the insert for $d = 12.6$ mm.

TABLE II

$TlMnCl_3$ ABSORPTION SPECTRUM AT 4.2°K IN THE REGION OF *C*- AND *D*-GROUP BANDS AND THEIR ASSIGNMENTS

Band	Frequency (cm^{-1})	Assignment[a]	Note
C_h	23,519	$\nu_E^{av} - \Delta_1$	Hot magnon sideband
C_0^a	23,568	ν_E^1 (^4E_g)	
C_0^b	23,578	ν_E^2 (^4E_g)	Pure excitonic band
C_1^a	23,601	$\nu_E^{av} + \Delta_2$	Cold magnon sideband
C_1^b	23,629	$\nu_E^{av} + \Delta_1$	
$C_1^{a,p}$	23,668	$C_1^a + \nu_p^1$	
$C_1^{b,p}$	23,696	$C_1^b + \nu_p^1$	Exciton–magnon–phonon sideband
$C_1^{a,2p}$	23,732	$C_1^a + 2\nu^1$	
C_2	23,747	$\nu_E^{av} + 173$	Three-magnon band
C_3	23,778	$\nu_A \rightarrow {}^4A_{1g}$	Pure excitonic band
C_4^a	23,825	$\nu_A + \Delta_1' + \mathrm{EMI}$[b]	Cold magnon sideband
C_4^b	23,840	$\nu_A + \Delta_3' + \mathrm{EMI}$	
$C_4^{a,p}$	23,889	$C_4^a + \nu_p^1$	Exciton–magnon–phonon sideband
C_5	23,930		
C_6	24,014		Phonon sideband
C_7	24,075		
C_8	24,119		
D_1	26,623	ν_D^1	Pure excitonic band
D_2	26,636	ν_D^2	
D_3	26,696	$\nu_D^{av} + \Delta_3$	
D_4	26,717		Cold magnon sideband
D_5	26,728	$\nu_D^{av} + 98$	
D_6	26,737		
D_7	26,755	$D_3 + \nu_p^2$	
D_8	26,765	$D_3 + \nu_p^1$	
D_9	26,796	$D_3 + \nu_p^3$	
D_{10}	26,820	$D_3 + \nu_p^4$	
D_{11}	26,868	$D_3 + \nu_p^5$	Exciton–magnon–phonon sideband
D_{12}	26,984	$D_3 + \nu_p^6$	
D_{13}	27,013	$D_5 + \nu_p^6$	
D_{14}	27,046	$D_{7,8} + \nu_p^6$	
D_{15}	27,113	$D_{10} + \nu_p^6$	
D_{16}	27,245	$D_3 + 2\nu_p^6$	

[a] Designations: $\Delta_1 = 56\ cm^{-1}$; $\Delta_2 = 28\ cm^{-1}$; $\Delta_1' = 47\ cm^{-1}$; $\Delta_3 = 66.5\ cm^{-1}$; $\Delta_3' = 62\ cm^{-1}$; $\nu_p^1 = 67\ cm^{-1}$; $\nu_p^2 = 59\ cm^{-1}$; $\nu_p^3 = 100\ cm^{-1}$; $\nu_p^4 = 124\ cm^{-1}$; $\nu_p^5 = 172\ cm^{-1}$; $\nu_p^6 = 283\ cm^{-1}$.

[b] EMI, exciton–magnon interaction.

been received from the analysis: $\Delta_1 = 56$, $\Delta_2 = 28$, and $\Delta_3 = 66.5\ cm^{-1}$.

The intensity of *D*-group bands does not increase on warming (Fig. 3). This result, like that in $RbMnF_3$ (*11*), shows no odd-parity vibronic origins. Odd-parity vibronic origin would cause a marked increase of the intensity ($f = f_0 \coth h\nu/2kT$; f_0 is the oscillator strength at zero temperature and ν is the effective frequency of the odd vibrations)

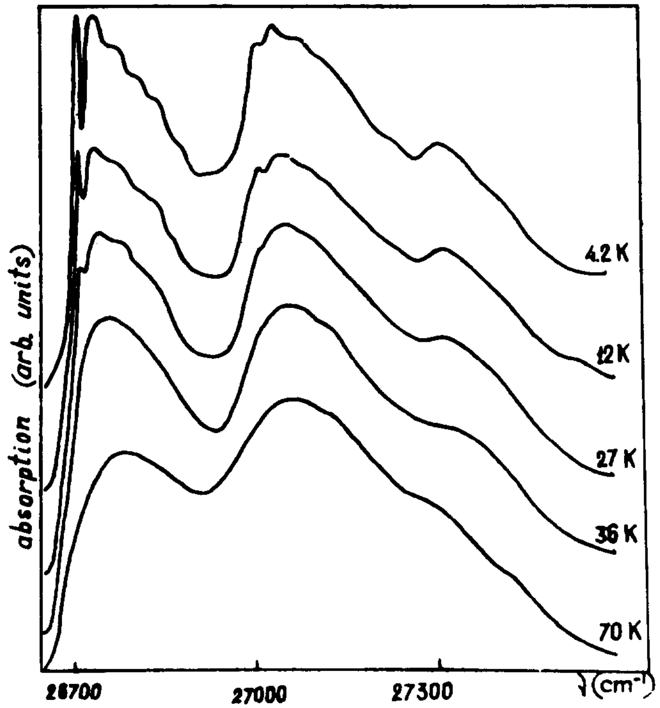

FIG. 3. Temperature dependence of the $TlMnCl_3$ absorption spectrum in the region of the D group; $d = 1.52$ mm.

but it has not been observed. D_3 is the origin of the D_7–D_{11} bands. As for other bands in the D group and the majority of bands in the C group, they form electron–vibrational series of the Eq. (1) type with $\nu_k = 283\ \text{cm}^{-1}$ for the D group and $\nu_k = 67\ \text{cm}^{-1}$ for the C group. EM bands are the origins of such series, which are typical for forbidden electronic transitions (*14*).

Phonon frequencies determined from the absorption spectrum are listed in Table II. Similar frequencies were determined by the Raman scattering experiment on $KMnF_3$ (*16*).

But the most interesting results are obtained from comparison of the intensity distribution versus the frequency for the C and D groups in $TlMnCl_3$ and $KMnF_3$. EM bands C_1–C_4 in the group of $KMnF_3$ have the highest intensity (*1, 3*), as is shown in Fig. 1. Other weak bands are EMP sidebands (*13*). Their influence on the intensity of the absorption spectrum at low temperatures is very small. Such EMP bands are separated from PE bands by more than $200\ \text{cm}^{-1}$ to the high-frequency region. As for $TlMnCl_3$ EMP bands are essential in the creation of its fine structure in the region from 0 to $200\ \text{cm}^{-1}$ ($\nu_p = 67\ \text{cm}^{-1}$) and give the main contribution to the intensity of the C group. D groups of $K(Rb)MnF_3$ and $TlMnCl_3$ have identical intensity–distribution dependences on the frequency [compare Fig. 2 with Fig. 14 from Ref. (*15*)] with EM bands of the highest intensity.

Following Ferguson (*14*), we explain such behavior using the Franck–Condon principle. In accordance with this principle an intensity distribution versus frequency depends on the displacement of the minimum of the potential energy curve for the excited state (r_e) away from the value of the configurational coordinate characteristic of the ground state (r_0). If $r_0 \approx r_e$, then electronic transition intensity is concentrated in the PE (or EM) transition as indicated in Fig. 4(*3*) because the vibrational overlap integral is the largest for such a transition. When $r_e > r_0$, a displacement of the minimum of the potential energy curve of the excited state takes place [Fig. 4(*2*)] and excitation of vibrations in the excited state occurs together with a shift of the position of maximum intensity in the spectrum from the PE (or EM) transition to energies which correspond to the excitation of a number of vibrational quanta in the excited state.

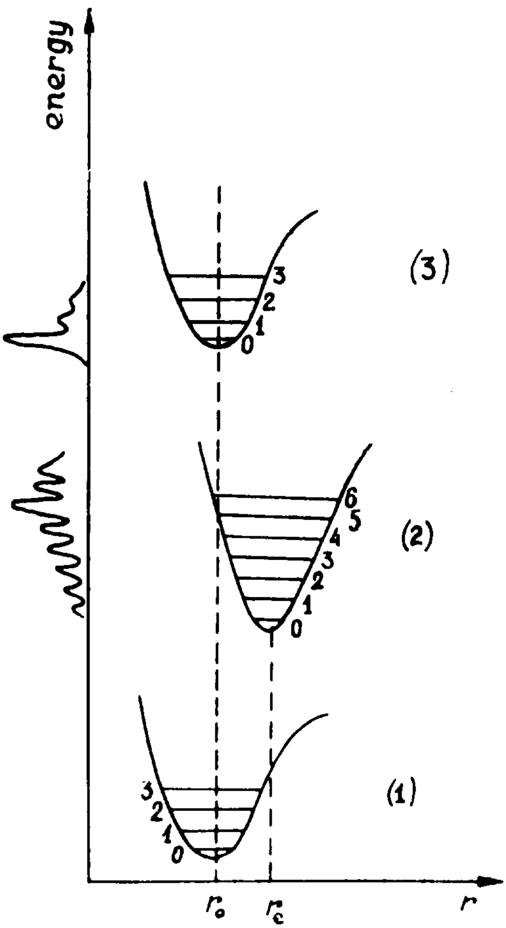

FIG. 4. Schematic picture of the electronic–vibrational transitions and intensity distributions for the different cases of the configurational coordinate changes: (1) ground state; (2) excited state with $r_e \gg r_0$; (3) excited state with $r_e \approx r_0$.

From Figs. 1 and 4 it can be seen that the situation of Fig. 4(*2*) occurs for the *C* group of $TlMnCl_3$ and the case of Fig. 4(*3*) takes place in fluorides (for example, in $KMnF_3$). Thus in $TlMnCl_3$ the site group of the Mn^{2+} excited state in the region of the *C* group has to be changed in comparison with the ground state.

For the *D* group an intensity distribution both for $TlMnCl_3$ and for $K(Rb)MnF_3$ is in accord with Fig 4(*3*) (compare with Fig. 3); therefore $r_0 \approx r_e$, and the site group of the excited state does not change.

Taking into account everything mentioned above, it becomes clear that the magnon–phonon interaction plays an essential role in the formation of the $TlMnCl_3$ absorption spectrum. $C_1^{a,p}$, $C_1^{b,p}$, $C_1^{a,2p}$, $C_4^{a,p}$ and D_7–D_{16} bands are the EMP sidebands of the ν_E^{av} and ν_D^{av} transitions. It is clear also that EMP and EM bands must have similar temperature dependences of frequencies and must differ in temperature variation of the phonon frequency. The appearance of the low-frequency magnons in the absorption spectrum of $TlMnCl_3$ may be caused by essential magnon–phonon interaction due to the close values of the magnon and phonon frequencies (Table II).

Acknowledgements

The author is grateful to K. S. Aleksandrov for his constant interest and support of the work, to A. I. Belyaeva and I. S. Edelman for useful discussions, to B. V. Beznosikov for kindly supplying $TlMnCl_3$ single crystals, and to E. A. Popov for technical assistance.

References

1. V. V. EREMENKO, "Vvedenie v opticheskuyu spekroskopiyu magnetikov," Naukova Dumka, Kiev (1975).
2. E. G. PETROV, "Teoriya magnitnukh eksitonov," Naukova Dumka, Kiev (1976).
3. A. I. BELYAEVA, Avtoreferat doktorskoi dissertasii, Physico–Technical Institute of Low Temperatures, Kharkov (1974).

4. A. I. BELYAEVA, M. M. KOTLYARSKII, AND I. S. EDELMAN, Preprint IPhSB–48Ph, Krasnoyarsk (1976).
5. I. S. EDELMAN, M. M. KOTLYARSKII, AND A. T. ANISTRATOV, *Phys. Status Solidi B* **70**, K15 (1975).
6. K. S. ALEKSANDROV, A. T. ANISTRATOV, A. I. KRUPNUI, L. A. POZDNYAKOVA, S. V. MELNIKOVA, AND B. V. BEZNOSIKOV, *Fiz. Tverd. Tela* **17**, 735 (1975).
7. N. V. FEDOSEEVA, I. P. SPEVAKOVA, B. V. BEZNOSIKOV, E. P. NAIDEN, AND V. A. KHOKHLOV, *Phys. Status Solidi A* **44**, 429 (1977).
8. V. I. SILAEV, A. I. BELYAEVA, AND M. M. KOTLYARSKII, *Prib. Tekh. Eksp.* **5**, 240 (1973); *Cryogenics* **14**, 405 (1974).
9. A. I. BELYAEVA AND M. M. KOTLYARSKII, *Phys. Status Solidi B* **76**, 419 (1976).
10. D. CURIE, C. BARTHOU, AND B. CANNY, *J. Chem. Phys.* **61**, 3048 (1974).
11. E. I. SOLOMON AND D. S. MCCLURE, *Phys. Rev. B* **9**, 4690 (1974.
12. J. FERGUSON, *Aust. J. Chem.* **21**, 307 (1968).
13. H. KOMURA, V. S. SRIVASTAVA, AND R. STEVENSON, *Phys. Rev. B* **8**, 377 (1973).
14. J. FERGUSON, *in* "Progress in Inorganic Chemistry" (S. J. LIPPARD, Ed.), Vol. 12, p. 159, Wiley–Interscience, New York (1970).
15. V. V. EREMENKO, V. P. NOVIKOV, AND E. G. PETROV, *Zh. Eksp. Teor. Fiz.* **66**, 2092 (1974).
16. YU. A. POPKOV, V. V. EREMENKO, AND V. P. PHOMIN, *Fiz. Tverd. Tela* **13**, 2028 (1971).